Multi-symplectic method for the coupled Schrödinger–KdV equations*

Zhang Hong(张 弘)[a], Song Song-He(宋松和)[a)b)†], Zhou Wei-En(周炜恩)[a], and Chen Xu-Dong(陈绪栋)[a]

[a] Department of Mathematics and System Science, College of Science, National University of Defense Technology, Changsha 410073, China
[b] State Key Laboratory of High Performance Computing, National University of Defense Technology, Changsha 410073, China

(Received 1 November 2013; revised manuscript received 11 February 2014; published online 10 June 2014)

In this paper, we present a multi-symplectic Hamiltonian formulation of the coupled Schrödinger-KdV equations (CSKE) with periodic boundary conditions. Then we develop a novel multi-symplectic Fourier pseudospectral (MSFP) scheme for the CSKE. In numerical experiments, we compare the MSFP method with the Crank–Nicholson (CN) method. Our results show high accuracy, effectiveness, and good ability of conserving the invariants of the MSFP method.

Keywords: coupled Schrödinger–KdV equations, multi-symplectic, Fourier pseudospectral method

PACS: 02.60.Cb, 02.70.Bf, 02.30.Jr **DOI:** 10.1088/1674-1056/23/8/080204

1. Introduction

In this paper, we consider the coupled Schrödinger–KdV equations (CSKE)

$$\begin{cases} \mathrm{i}\varepsilon E_t + \dfrac{3}{2}E_{xx} - \dfrac{1}{2}NE = 0, \\ (x,t) \in R \times (0,T], \\ N_t + \dfrac{N_{xxx}}{2} + \dfrac{1}{2}(N^2 + |E|^2)_x = 0, \\ (x,t) \in R \times (0,T], \end{cases} \tag{1}$$

with the initial value and periodic boundary conditions

$$\begin{aligned} &E(x,t) = E(x+l,t), \quad N(x,t) = N(x+l,t), \\ &(x,t) \in R \times (0,T], \\ &E(x,0) = E_0(x), \quad N(x,0) = N_0(x), \end{aligned} \tag{2}$$

where $E_0(x)$ and $N_0(x)$ are known l-periodic functions, $l > 0$. The proof for the existence of the solution of the CSKE is presented in Ref. [1]

The CSKE is the model describing nonlinear dynamics of one-dimensional Langmuir and ion-acoustic waves in a system of coordinates moving at the ion-acoustic speed. Here E is a complex function describing an electric field of Langmuir oscillations and N is a real function describing low-frequency density perturbation, $\varepsilon > 0$ is a constant. In the CSKE (1), the first equation is called the electric field equation and the second is the density equation. The initial value and periodic boundary condition problem for the CSKE (1) has the following invariants:[2]

(i) the number of Langmuir plasmons

$$I_1(t) = \int_0^l |E|^2 \mathrm{d}x = \int_0^l |E_0|^2 \mathrm{d}x = I_1(0), \quad t \geq 0; \tag{3}$$

(ii) the number of particles

$$I_2 = \int_0^l N \mathrm{d}x = \int_0^l N_0 \mathrm{d}x = I_2(0), \quad t \geq 0; \tag{4}$$

(iii) the energy of the oscillations

$$\begin{aligned} I_3 &= \int_0^l 3|E_x|^2 + |E|^2 N + \frac{N^3}{3} - \frac{1}{2}(N_x)^2 \mathrm{d}x \\ &= I_3(0), \quad t \geq 0. \end{aligned} \tag{5}$$

These invariants play important roles in physical theories, and are useful tools for qualitative analysis.

The CSKE has been studied for many years and the analytical solution of the CSKE has been presented in Refs. [3]–[7]. Results on existence, uniqueness of the solution, and global attractor of this system have been presented in Refs. [1] and [8]. Recently, various methods, for example, the variational iteration method,[9] the decomposition method,[10] and the ansatz method[11] have been used to solve this problem.

In order to solve the CSKE numerically, Appert *et al.*[2] used the explicit three-time-level Zabusky–Kruskal scheme for the density equation and a standard Crank–Nicholson scheme for the electric field equation, Bai *et al.*[12] proposed the finite element method for the CSKE, Golbabai *et al.*[13] used the radial basis function method, and Liu *et al.*[14] studied an element-free Galerkin method to solve the CSKE.

In this paper, we propose a multi-symplectic method to find the solution of the CSKE. In recent decades, multi-symplectic methods[15] have been widely used to solve Hamiltonian partial differential equations (PDEs), such as nonlinear Schrödinger equations,[16–19] Klein–Gordon–Zakharov equations,[20,21] Ito-type coupled KdV equations,[22] and the Zakharov–Kuznetsov equation.[23] Until now, to the best

*Project supported by the National Natural Science Foundation of China (Grant No. 91130013) and the Open Foundation of State Key Laboratory of High Performance Computing.

†Corresponding author. E-mail: shsong@nudt.edu.cn

© 2014 Chinese Physical Society and IOP Publishing Ltd

of our knowledge, the methods that preserve the multi-symplectic structure of the CSKE have not been found. Therefore, it is of great interests to develop a multi-symplectic scheme for solving the CSKE.

The rest of the paper is organized as follows. In Section 2, we construct the multi-symplectic Hamiltonian formulation of the CSKE, and give some corresponding local conservation laws. Section 3 is devoted to presenting a multi-symplectic Fourier pseudospectral (MSFP) method by using the Fourier pseudospectral method in space discretization and an implicit midpoint rule in time discretization. In Section 4, numerical experiments of the CSKE are presented to show the effectiveness of the proposed multi-symplectic method. The last section is our conclusion.

2. Multi-symplectic formulation of the CSKE

By writing $E = p + \mathrm{i}q$, the CSKE (1) can be written as a system of real-value equations

$$\begin{cases} \varepsilon p_t = -\dfrac{3}{2}q_{xx} + \dfrac{1}{2}Nq, \\ N_t = -\dfrac{1}{2}N_{xxx} - \dfrac{1}{2}(p^2+q^2+N^2)_x, \\ \varepsilon q_t = \dfrac{3}{2}p_{xx} - \dfrac{1}{2}Np. \end{cases} \tag{6}$$

By introducing new variables f, g, h, v, and w, which satisfy $N = f_x$, $g = N_x$, $h_x = -\frac{1}{2}N_t$, $v = p_x$, and $w = q_x$, we obtain the first-order system as follows:

$$\begin{cases} -2\varepsilon q_t + 3v_x = Np, \\ 2\varepsilon p_t + 3w_x = Nq, \\ \dfrac{1}{2}N_t + h_x = 0, \\ -\dfrac{1}{2}f_t - \dfrac{1}{2}g_x = -h + \dfrac{1}{2}(N^2+p^2+q^2), \\ \dfrac{1}{2}N_x = \dfrac{1}{2}g, \\ -f_x = -N, \\ -3p_x = -3v, \\ -3q_x = -3w. \end{cases} \tag{7}$$

System (7) can be written as the multi-symplectic form

$$Mz_t + Kz_x = \nabla_z S(z), \tag{8}$$

with state variable

$$z = [p,\ q,\ f,\ N,\ g,\ h,\ v,\ w]^{\mathrm{T}},$$

$$M = \begin{bmatrix} J_1 & 0 \\ 0 & 0 \end{bmatrix},$$

$$K = \begin{bmatrix} 0 & J_2 \\ -J_2^{\mathrm{T}} & 0 \end{bmatrix},$$

and the Hamiltonian function is

$$S(z) = \frac{1}{2}(p^2+q^2)N + \frac{1}{6}N^3 - hN + \frac{1}{4}g^2 - \frac{3}{2}(v^2+w^2),$$

where

$$J_1 = \begin{bmatrix} 0 & -2\varepsilon & 0 & 0 \\ 2\varepsilon & 0 & 0 & 0 \\ 0 & 0 & 0 & -\dfrac{1}{2} \\ 0 & 0 & \dfrac{1}{2} & 0 \end{bmatrix},$$

$$J_2 = \begin{bmatrix} 0 & 0 & 3 & 0 \\ 0 & 0 & 0 & 3 \\ 0 & 1 & 0 & 0 \\ -\dfrac{1}{2} & 0 & 0 & 0 \end{bmatrix}.$$

The multi-symplectic Hamiltonian system (8) has a multi-symplectic conservation law[15,24]

$$\frac{\partial}{\partial t}\omega + \frac{\partial}{\partial x}\kappa = 0, \tag{9}$$

where ω and κ are the pre-symplectic form

$$\omega = \frac{1}{2}\mathrm{d}z \wedge M\mathrm{d}z, \quad \kappa = \frac{1}{2}\mathrm{d}z \wedge K\mathrm{d}z.$$

The system (8) has an energy conservation law (ECL)

$$\frac{\partial}{\partial t}E + \frac{\partial}{\partial x}F = 0, \tag{10}$$

with energy density

$$E = S(z) - \frac{1}{2}z^{\mathrm{T}}Kz_x,$$

and energy flux

$$F = \frac{1}{2}z^{\mathrm{T}}Kz_t.$$

The system (8) also has a momentum conservation law (MCL)

$$\frac{\partial}{\partial t}I + \frac{\partial}{\partial x}G = 0, \tag{11}$$

with momentum density

$$I = \frac{1}{2}z^{\mathrm{T}}Mz_x,$$

and momentum flux

$$G = S(z) - \frac{1}{2}z^{\mathrm{T}}Mz_t.$$

For the CSKE (1), the corresponding multi-symplectic conservation law is

$$\frac{\partial}{\partial t}\left(2\varepsilon\,\mathrm{d}q\wedge\mathrm{d}p + \frac{1}{2}\mathrm{d}f\wedge\mathrm{d}N\right) + \frac{\partial}{\partial x}\left(3\,\mathrm{d}p\wedge\mathrm{d}N + 3\,\mathrm{d}q\wedge\mathrm{d}w + \mathrm{d}f\wedge\mathrm{d}h + \frac{1}{2}\mathrm{d}g\wedge\mathrm{d}N\right) = 0. \tag{12}$$

The corresponding energy conservation law is

$$\frac{\partial}{\partial t}\left(\frac{1}{2}(p^2+q^2)N + \frac{1}{6}N^3 - \frac{1}{4}g^2 + \frac{3}{2}(v^2+w^2)\right) + \frac{\partial}{\partial x}\left(\frac{3}{2}pv_t - \frac{3}{2}vp_t + \frac{3}{2}qw_t - \frac{3}{2}wq_t + \frac{1}{2}fh_t\right.$$

$$-\frac{1}{2}hf_t+\frac{1}{4}gN_t-\frac{1}{4}Ng_t\Big)=0. \tag{13}$$

The corresponding momentum conservation law is

$$\begin{aligned}&\frac{\partial}{\partial t}\Big(\varepsilon qv-\varepsilon pw+\frac{1}{2}fg\Big)+\frac{\partial}{\partial x}\Big(\frac{1}{2}(p^2+q^2)N\\&+\frac{1}{6}N^3-hN+\frac{1}{4}g^2-\frac{3}{2}(v^2+w^2)+\varepsilon pq_t-\varepsilon qp_t\\&-\frac{1}{4}fN_t+\frac{1}{4}Nf_t\Big)=0.\end{aligned} \tag{14}$$

Under periodic boundary conditions, the above local conservation laws (12)–(14) can be integrated in the x direction to obtain the global conservation laws[15,24,25] as follows:

i) conservation of global symplecticity:

$$\frac{\mathrm{d}}{\mathrm{d}t}\int_0^l \omega(z)\,\mathrm{d}x=0; \tag{15}$$

ii) conservation of global energy:

$$\frac{\mathrm{d}}{\mathrm{d}t}\int_0^1 E(z)\,\mathrm{d}x=0; \tag{16}$$

iii) conservation of global momentum:

$$\frac{\mathrm{d}}{\mathrm{d}t}\int_0^1 I(z)\,\mathrm{d}x=0. \tag{17}$$

We note that the global conservation of energy (16) or momentum (17) is necessary but not sufficient for the local conservation of energy or momentum.

3. Multi-symplectic Fourier pseudospectral method for the CSKE

It has been verified that appropriate Fourier pseudospectral discretization in space for the multi-symplectic form of the Schrödinger equation and KdV equation with periodic boundary conditions can preserve the multi-symplectic conservation laws unchanged. Therefore, we think a Fourier pseduospectral method can still preserve the multi-symplectic conservation law of the CSKE.

It is noticed that the first-order partial differential operator $\partial/\partial x$ yields the Fourier spectral differentiation matrix D_1, here D_1 is an $N\times N$ (N is even) skew-symmetric matrix with elements

$$(D_1)_{j+1,l+1}=\begin{cases}\frac{1}{2}(-1)^{j+l}\mu\cot\Big(\mu\frac{x_j-x_l}{2}\Big), & j\neq l,\\ 0, & j=l,\end{cases}$$

for $\quad j,l=0,1,\ldots,N-1,$

where $\mu=2\pi/L$. For more details, see Ref. [16] and the references therein.

We apply the Fourier pseudospectral method to discretize the multi-symplectic system (19) in space and using the notations

$$\bar{p}^n=[p_0^n,p_1^n,\ldots,p_{N-1}^n]^{\mathrm{T}}, \tag{18}$$

$\bar{q}$, $\bar{f}$, $\bar{N}$, $\bar{g}$, $\bar{h}$, $\bar{v}$, and $\bar{w}$ are similar to $\bar{p}$.

Then we can discretize the system (19) with respect to time by any multi-symplectic integrators, for example, the multi-symplectic Preissman scheme or the implicit midpoint rule. Due to the simplicity and effectivity, we choose the implicit midpoint rule and obtain the discrete system

$$\begin{cases}-2\varepsilon D_t\bar{q}^n+3D_1A_t\bar{v}^n=(A_t\bar{N}^n)(A_t\bar{p}^n),\\ 2\varepsilon D_t\bar{p}^n+3D_1A_t\bar{w}^n=(A_t\bar{N}^n)(A_t\bar{q}^n),\\ \frac{1}{2}D_t\bar{N}^n+D_1A_t\bar{h}^n=0,\\ -\frac{1}{2}D_t\bar{f}^n-\frac{1}{2}D_1A_t\bar{g}^n\\ =-A_t\bar{h}^n+\frac{1}{2}(A_t\bar{N}^n)^2+\frac{1}{2}((A_t\bar{p}^n)^2+(A_t\bar{q}^n)^2),\\ \frac{1}{2}D_1A_t\bar{N}^n=\frac{1}{2}A_t\bar{g}^n,\\ -D_1A_t\bar{f}^n=-A_t\bar{N}^n,\\ -3D_1A_t\bar{p}^n=-3A_t\bar{v}^n,\\ -3D_1A_t\bar{q}^n=-3A_t\bar{w}^n,\end{cases} \tag{19}$$

here Δt is the time step, $D_t\bar{p}^n=(\bar{p}^{n+1}-\bar{p}^n)/\Delta t$ is the difference operator, $A_t\bar{p}^n=(\bar{p}^{n+1}+\bar{p}^n)/2$ is the average operator in time, D_1 is the first order Fourier spectral differentiation matrix, $(\bar{p}^n)^2=[p_0^np_0^n,\ p_1^np_1^n,\ \ldots,\ p_{N-1}^np_{N-1}^n]^{\mathrm{T}}$, and others that are similar respectively.

Eliminating the variables $f,g,h,v,andw$, we can obtain the following multi-symplectic Fourier pseudospectral method for the CSKE (1)

$$\begin{cases}\varepsilon D_t\bar{p}^n=-\frac{3}{2}A_tD_1^2\bar{q}^n+\frac{1}{2}(A_t\bar{q}^n)(A_t\bar{N}^n),\\ D_tA_t\bar{N}^n=-\frac{1}{2}A_tD_1^3A_t\bar{N}^n-\frac{1}{2}A_tD_1((A_t\bar{p}^n)^2\\ \quad+(A_t\bar{q}^n)^2+(A_t\bar{N}^n)^2),\\ \varepsilon D_t\bar{q}^n=\frac{3}{2}A_tD_1^2\bar{p}^n-\frac{1}{2}(A_t\bar{p}^n)(A_t\bar{N}^n).\end{cases} \tag{20}$$

The three-level scheme (20) is equivalent to the following two-level scheme

$$\begin{cases}\varepsilon D_t\bar{p}^n=-\frac{3}{2}A_tD_1^2\bar{q}^n+\frac{1}{2}(A_t\bar{q}^n)(A_t\bar{N}^n),\\ D_t\bar{N}^n=-\frac{1}{2}D_1^3A_t\bar{N}^n-\frac{1}{2}D_1((A_t\bar{p}^n)^2\\ \quad+(A_t\bar{q}^n)^2+(A_t\bar{N}^n)^2),\\ \varepsilon D_t\bar{q}^n=\frac{3}{2}A_tD_1^2\bar{p}^n-\frac{1}{2}(A_t\bar{p}^n)(A_t\bar{N}^n).\end{cases} \tag{21}$$

We can use the fixed point iteration method to solve the nonlinear system.

4. Numerical experiments

In this section, we present some numerical results obtained by the MSFP method presented in the previous section. The main issues are the accuracy, the discrete invariants, and the long simulation time. The accuracy of our MSFP method is tested by looking at the error using the L_2 norm

$$L_2 = \|u-\bar{u}\|_2 = \left(\Delta x \sum_{j=0}^{N-1}(u_j-\bar{u}_j)^2\right)^{1/2}, \tag{22}$$

where Δx is the spatial step size, N is the number of points, and $\bar{u}$ is the discrete solution.

Example 1 The authors in Ref. [8] derived a stationary traveling localized solution to the CSKE (1), the C-soliton given by

$$E(x,t) = -\frac{6}{5}\sqrt{3}\alpha\,\mathrm{sech}(\xi)\tanh(\xi) \times \exp\left(\mathrm{i}\alpha\left(\frac{3}{20\varepsilon}-\frac{\varepsilon\alpha}{6}\right)t-\frac{\varepsilon x}{3}\right), \tag{23}$$

$$N(x,t) = -\frac{9}{5}\alpha\,\mathrm{sech}^2(\xi), \tag{24}$$

where $\xi=(\alpha/10)^{1/2}(x+\alpha t)$, α is a free positive parameter. We take the value of the exact solutions (23) and (24) at $t=0$ as our initial conditions:

$$E_0 = -\frac{6}{5}\sqrt{3}\alpha\,\mathrm{sech}(\xi)\tanh(\xi)\exp\left[\mathrm{i}\alpha\left(-\frac{\varepsilon x}{3}\right)\right], \tag{25}$$

$$N_0 = -\frac{9}{5}\alpha\,\mathrm{sech}^2(\xi), \tag{26}$$

where $\xi=(\alpha/10)^{1/2}x$.

We choose the parameters $\varepsilon=1$, $\alpha=0.45$, then solve this problem with the time step $\Delta t=1\times10^{-4}$, the spatial interval $[-30,30]$, and the spatial step size $\Delta x=0.25$. We compare the MSFP method with the Crank–Nicolson (CN) method,[2] and show the results in Tables 1–4. From these tables, we can see that the MSFP method is much better than the CN method.

Table 1. Comparison of MSFP with CN and the exact solution for p, at $t=1\times10^{-3}$, $\Delta t=1\times10^{-4}$, $\Delta x=0.25$.

x	MSFP	CN	Exact solution
–20	-2.6597×10^{-2}	-2.6616×10^{-2}	-2.6597×10^{-2}
–10	1.5188×10^{-2}	1.5950×10^{-2}	1.5188×10^{-2}
0	-8.9430×10^{-5}	5.2367×10^{-5}	-8.9284×10^{-5}
10	-1.5200×10^{-2}	-1.5952×10^{-2}	-1.5200×10^{-2}
20	2.6592×10^{-2}	2.6626×10^{-2}	2.6592×10^{-2}

Table 2. Comparison of MSFP with CN and the exact solution for q, at $t=1\times10^{-3}$, $\Delta t=1\times10^{-4}$, $\Delta x=0.25$.

x	MSFP	CN	Exact solution
–20	3.7898×10^{-3}	3.8986×10^{-3}	3.7904×10^{-3}
–10	2.1428×10^{-1}	2.1445×10^{-1}	2.1428×10^{-1}
0	-6.5360×10^{-7}	3.5376×10^{-3}	3.0133×10^{-9}
10	2.1424×10^{-1}	2.1425×10^{-1}	2.1424×10^{-1}
20	3.7909×10^{-3}	3.8986×10^{-3}	3.7915×10^{-3}

Table 3. Comparison of MSFP with CN and the exact solution for N, at $t=1\times10^{-3}$, $\Delta t=1\times10^{-4}$, $\Delta x=0.25$.

x	MSFP	CN	Exact solution
–20	-6.6886×10^{-4}	-6.7188×10^{-4}	-6.6886×10^{-4}
–10	-4.5256×10^{-2}	-4.5448×10^{-2}	-4.5256×10^{-2}
0	-8.1000×10^{-1}	-8.1000×10^{-1}	-8.1000×10^{-1}
10	-4.5239×10^{-2}	-4.5048×10^{-2}	-4.5239×10^{-2}
20	-6.6861×10^{-4}	-6.6560×10^{-4}	-6.6861×10^{-4}

Table 4. Comparison of L_2 errors for the numerical solution at $t=1\times10^{-3}$, $\Delta t=1\times10^{-4}$, $\Delta x=0.25$.

	L_2 (MSFP)	L_2 (CN)
p	7.5939×10^{-6}	3.4776×10^{-3}
q	3.8278×10^{-5}	2.0203×10^{-3}
N	1.0328×10^{-7}	3.3631×10^{-4}

In Fig. 1 we plot the evolution of the numerical solution of p, q, $|E|$, N from $t=0$ to $t=10$ with $\Delta t=0.1$, $\Delta x=0.5$. The absolute errors of the invariants I_1, I_2, and I_3 are plotted in Fig. 2. From Fig. 1, we can see that the motion of the solitary waves is well simulated after the long calculation time, and the oscillatory phenomenon has not appeared. Figure 2 shows that the multi-symplectic scheme conserves the number of Langmuir plasmons, the number of particles, and the energy of the oscillations.

From the tables and figures, we can conclude that the MSFP method can solve the CSKE (1) accurately, and it is much better than the CN method.

Example 2 The model equations for the CSKE can also be solved in the following form[14]

$$\begin{cases} \mathrm{i}E_t = E_{xx}+NE, \\ N_t+6NN_x+N_{xxx}=(|E|^2)_x, \end{cases} \tag{27}$$

the initial and boundary conditions are the same as those in Eq. (2). The exact solution is given[26] by

$$E(x,t) = \mathrm{e}^{\mathrm{i}\theta}(-\sqrt{2}(2c_2\pm\delta)+6\sqrt{2}c_2\,\mathrm{sech}^2(\sqrt{c_2}\xi)), \tag{28}$$

$$N(x,t) = -\frac{1}{3}(\gamma+6c_2\pm\delta)+6c_2\,\mathrm{sech}^2(\sqrt{c_2}\xi), \tag{29}$$

where $\xi=x+2\gamma t$, $\theta=\gamma x+(\gamma+3\gamma^2\pm\delta)t/3$, and

$$\delta=\sqrt{\sqrt{2}c_1c_3+4c_2^2}.$$

c_1, c_3, and $c_2>0$ are arbitrary constants. The CSKE (27) has also been solved in Ref. [14] by using an element-free Galerkin (EFG) method. As the same with Ref. [14], we choose $c_1=c_3=0$. For the CSKE (27), the first two invariants are the same as I_1 and I_2, but the third invariant is

$$I_3' = \int\frac{1}{2}\left(-|E_x|^2+|E|^2N+\frac{1}{4}N_x^2-\frac{N^3}{2}\right)\mathrm{d}x. \tag{30}$$

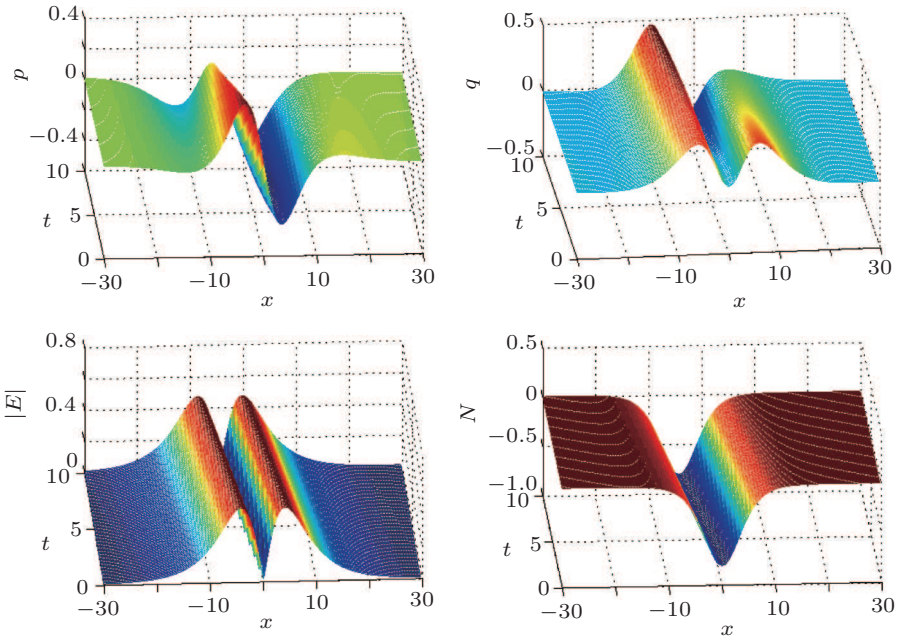


Fig. 1. (color online) Evolution of the MSFP solution from $t = 0$ to $t = 10$, $\Delta t = 0.1$, $\Delta x = 0.5$.

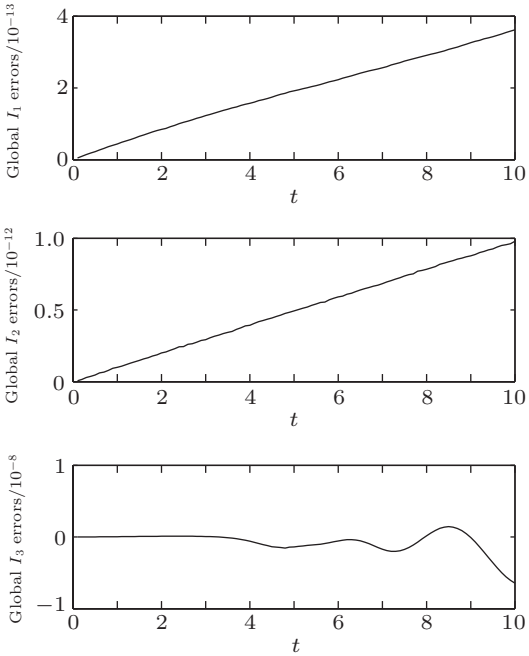


Fig. 2. Global errors of the three invariants obtained by the MSFP method, from $t = 0$ to $t = 10$, $\Delta t = 0.1$, $\Delta x = 0.5$.

The CSKE (27) can also be written in the multi-symplectic form with state variable

$$z = [p,\ q,\ f,\ N,\ g,\ h,\ v,\ w]^{\mathrm{T}},$$
$$M = \begin{bmatrix} J_1' & 0 \\ 0 & 0 \end{bmatrix}, \quad K = \begin{bmatrix} 0 & J_2' \\ -J_2'^{T} & 0 \end{bmatrix},$$

and the Hamiltonian function is

$$S(z) = \frac{1}{2}(p^2+q^2)N + N^3 - hN + \frac{1}{2}g^2 - \frac{1}{2}(v^2+w^2),$$

where

$$J_1' = \begin{bmatrix} 0 & -1 & 0 & 0 \\ 1 & 0 & 0 & 0 \\ 0 & 0 & 0 & \frac{1}{2} \\ 0 & 0 & -\frac{1}{2} & 0 \end{bmatrix}, \quad J_2' = \begin{bmatrix} 0 & 0 & -1 & 0 \\ 0 & 0 & 0 & -1 \\ 0 & 1 & 0 & 0 \\ -1 & 0 & 0 & 0 \end{bmatrix}.$$

By using the Fourier pseudospectral method in space discretizaiton and the midpoint rule with respect to time, we can get the three-level MSFP scheme for the CSKE (27)

$$\begin{cases} \bar{p}^n = A_t D_1^2 \bar{q}^n + (A_t \bar{q}^n)(A_t \bar{N}^n), \\ D_t A_t \bar{N}^n = -A_t D_1^3 A_t \bar{N}^n + A_t D_1((A_t \bar{p}^n)^2 \\ \quad + (A_t \bar{q}^n)^2 - 3(A_t \bar{N}^n)^2), \\ D_t \bar{q}^n = -A_t D_1^2 \bar{p}^n - (A_t \bar{p}^n)(A_t \bar{N}^n). \end{cases} \tag{31}$$

The scheme (31) is equivalent to the following two-level scheme

$$\begin{cases} D_t \bar{p}^n = A_t D_1^2 \bar{q}^n + (A_t \bar{q}^n)(A_t \bar{N}^n), \\ D_t \bar{N}^n = -D_1^3 A_t \bar{N}^n + D_1((A_t \bar{p}^n)^2 \\ \quad + (A_t \bar{q}^n)^2 - 3(A_t \bar{N}^n)^2), \\ D_t \bar{q}^n = -A_t D_1^2 \bar{p}^n - (A_t \bar{p}^n)(A_t \bar{N}^n). \end{cases} \tag{32}$$

In this example, computations were done with the time step $\Delta t = 0.01$, the spatial interval $[-30, 30]$, and the spatial step size $\Delta x = 0.25$. In Fig. 3, we plot the numerical results obtained by the MSFP method and the exact solution at $t = 1$ with $c_2 = 0.01$ and $\gamma = 0.1$; in Fig. 4, we plot the corresponding absolute errors of the invariants I_1, I_2, and I_3'. In Fig. 5, we show the numerical solution obtained by the MSFP method and the exact solution with $c_2 = 0.01$ and $\gamma = 1$; in Fig. 6, we plot the corresponding errors of the invariants.

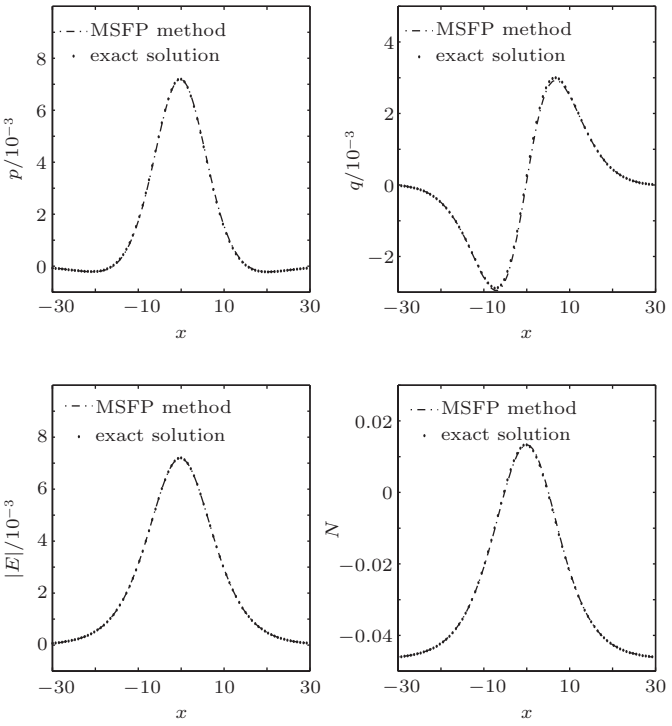


Fig. 3. Numerical solution and exact solution at $t = 1$, $\Delta t = 0.01$, $\Delta x = 0.25$, $c_2 = 0.01$, and $\gamma = 0.1$.

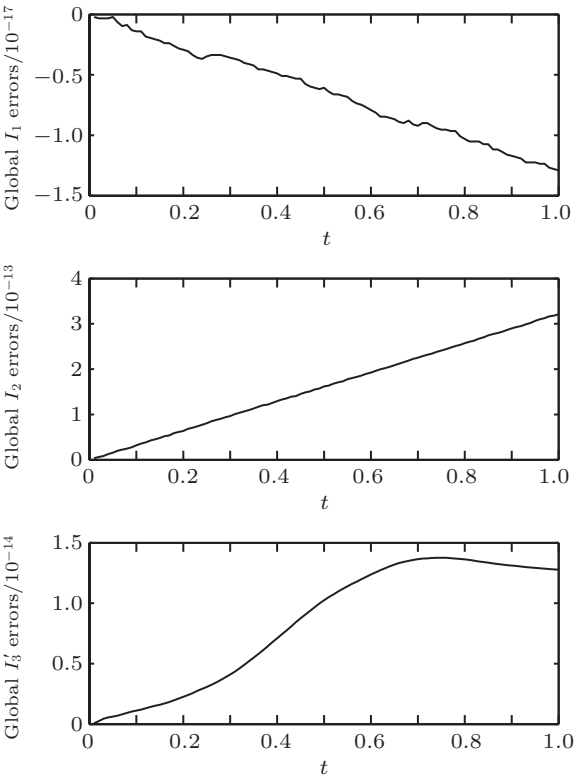


Fig. 4. Global errors of I_1, I_2, and I_3' obtained by the MSFP method, from $t = 0$ to $t = 1$, $\Delta t = 0.01$, $\Delta x = 0.25$, $c_2 = 0.01$, and $\gamma = 0.1$.

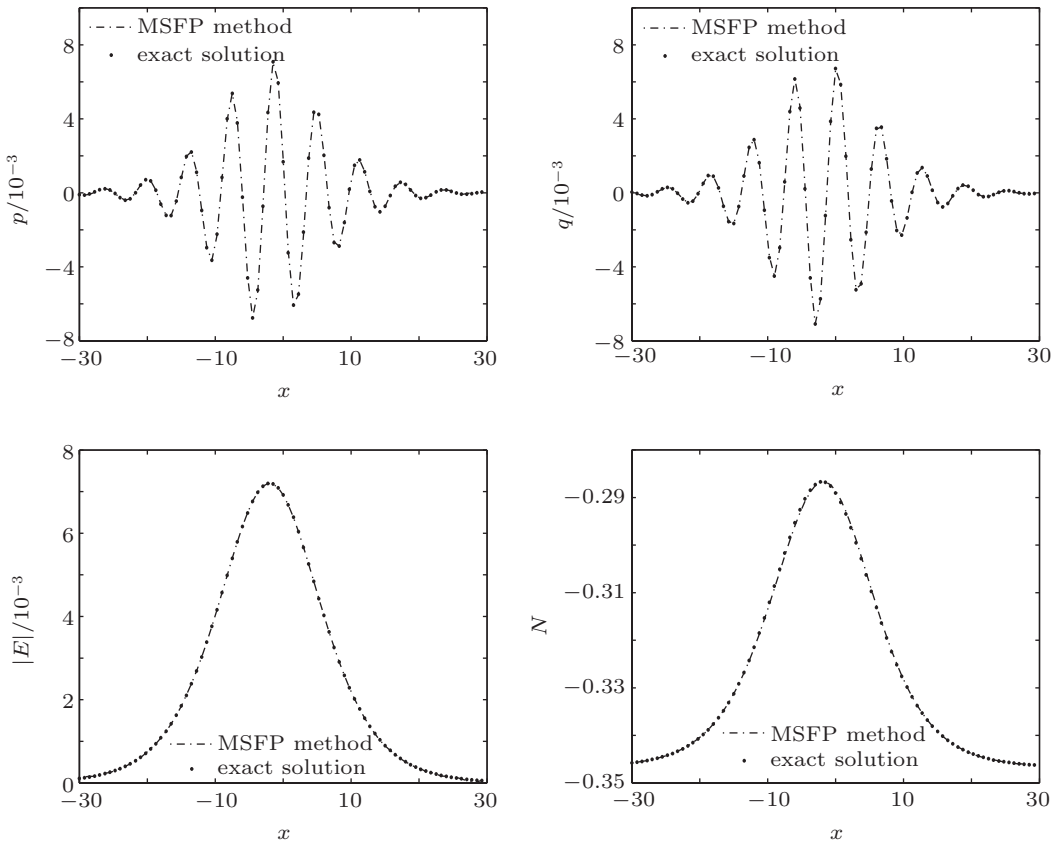


Fig. 5. Numerical solution and exact solution at $t = 1$, $\Delta t = 0.01$, $\Delta x = 0.25$, $c_2 = 0.01$, $\gamma = 1$.

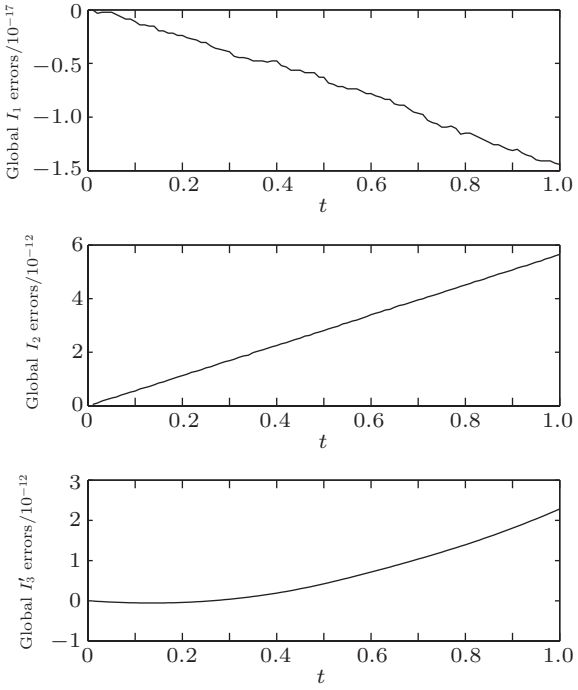


Fig. 6. Global errors of I_1, I_2, and I_3' obtained by the MSFP method, from $t = 0$ to $t = 1$, $\Delta t = 0.01$, $\Delta x = 0.25$, $c_2 = 0.01$, and $\gamma = 1$.

From Figs. 3–6, we can draw the conclusion that the MSFP method can provide a highly accurate solution for the CSKE (27).

5. Conclusions

In this paper, we consider the coupled Schrödinger–KdV equations from the aspect of multi-symplectic methods. The three conservation laws of the multi-symplectic method are the most important advantages of this scheme over the traditional difference methods or the finite element methods. The accuracy of this method is verified by making comparisons with the CN method. The numerical results show that the proposed scheme can also keep the invariants well, which is of great importance in simulations.

Acknowledgments

The authors acknowledge the valuable comments of the referees and their helpful discussion with Dr. Qian Xu.

References

[1] Guo B and Chen F 1997 *Nonlinear Anal. Theory Methods Appl.* **29** 569
[2] Appert K and Vaclavik J 1977 *Phys. Fluids* **20** 1845
[3] Nishikawa K, Hojo H, Mima K and Ikeze H 1974 *Phys. Rev. Lett.* **33** 148
[4] Mahankov V G 1978 *Phys. Rep.* **35** 1
[5] Gibbous J 1977 *J. Plasma Phys.* **17** 153
[6] Albert J and Pava J A 2003 *Proc. R. Soc. Edinburgh* **133** 987
[7] Peng Y Z 2004 *Pramana* **62** 933
[8] Guo B and Shen L 1982 *Proceedings of DD-3 Symposium*, August 23–September 16, 1982, Changchun, China, p. 417
[9] Abdou M A and Sdiman A A 2005 *Physica D* **211** 1
[10] Kaya D 2003 *Phys. Lett. A* **313** 82
[11] Labidi M, Ebadi G, Zerrad E and Biswas A 2012 *Pramana.* **78** 59
[12] Bai D and Zhang L 2009 *Phys. Lett. A* **373** 2237
[13] Golbabai A and Safdari-Baighani A 2011 *Computing* **92** 225
[14] Liu Y Q, Cheng R J and Ge H X 2013 *Chin. Phys. B* **22** 100204
[15] Bridges T J and Reich S 2001 *Phys. Lett. A* **284** 184
[16] Chen J B, Qin M Z and Tang Y F 2002 *Comput. Math. Appl.* **43** 1095
[17] Huang L Y 2009 *Chin. J. Comput. Phys.* **26** 693
[18] Wang Y S, Li Q H and Song Y Z 2008 *Chin. Phys. Lett.* **25** 1538
[19] Kong L H, Hong J L, Wang L and Fu F F 2009 *J. Comput. Appl. Math.* **231** 664
[20] Wang J 2009 *J. Phys. A: Math. Theor.* **42** 085205
[21] Cai J X and Liang H 2012 *Chin. Phys. Lett.* **29** 080201
[22] Chen Y M, Song S H and Zhu H J 2012 *Appl. Math. Comput.* **218** 5552
[23] Qian X, Song S H, Gao E and Li W B 2012 *Chin. Phys. B* **21** 070206
[24] Reich S 2000 *J. Comput. Phys.* **157** 473
[25] Dehghan M and Shokri A 2008 *Math. Comput. Simul.* **79** 700
[26] Fan E G 2002 *J. Phys. A: Math. Gen.* **35** 6853